Infection assays in *Arabidopsis* reveal candidate effectors from the poplar rust fungus that promote susceptibility to bacteria and oomycete pathogens

Hugo Germain[1, 2Ψ], David L. Joly[3], Caroline Mireault[1], Mélodie B. Plourde[1], Claire Letanneur[1], Donald Stewart[2], Marie-Josée Morency[2], Benjamin Petre[4,5], Sébastien Duplessis[5], Armand Séguin[2].

(1) Department of Chemistry, Biochemistry and Physics, Université du Québec à Trois-Rivières, 3351 boul. des Forges, Trois-Rivières, QC, G9A 5H7, Canada

(2) Natural Resources Canada, Canadian Forest Service, Laurentian Forestry Centre, 1055 du P.E.P.S., P.O. Box 10380, Stn. Sainte-Foy, Québec, QC, G1V 4C7, Canada

(3) Département de biologie, Université de Moncton, 18 avenue Antonine-Maillet, Moncton, NB, E1A 3E9, Canada

(4) The Sainsbury Laboratory, Norwich Research Park, Norwich, NR4 7UH, United Kingdom

(5) INRA, UMR 1136 Interactions Arbres/Microorganismes, INRA/Université de Lorraine, Centre INRA Nancy Lorraine, 54280 Champenoux, France

HG:Hugo.Germain@uqtr.ca
DLJ: David.Joly@umoncton.ca
CM: Caroline.Mireault@uqtr.ca
MBP : Melodie.Bplourde@uqtr.ca
CL : Claire.Letanneur@uqtr.ca
DS: Don.Stewart@canada.gc.ca
MJM: Marie-Josee.Morency@canada.gc.ca
BP: benjpetre@gmail.com

This article has been accepted for publication and undergone full peer review but has not been through the copyediting, typesetting, pagination and proofreading process which may lead to differences between this version and the Version of Record. Please cite this article as an 'Accepted Article', doi: 10.1111/mpp.12514

SD: Sebastien.Duplessis@inra.fr
AS: Armand.Seguin@canada.gc.ca

Ψ Author for correspondence: Hugo Germain
Tel: 819-376-5011
Email: Hugo.Germain@uqtr.ca

Word number: 5382

Abstract

Fungi of the Pucciniales order cause rust diseases, which altogether affect thousands of plant species worldwide and pose major threat to several crops. How rust effectors - virulence proteins delivered into infected tissues to modulate host functions - contribute to pathogen virulence remains poorly understood. *Melampsora larici-populina* is a devastating and widespread rust pathogen of poplars and its genome encodes 1,184 identified small secreted proteins that could potentially act as effectors. Here, following specific criteria we selected 16 candidate effector proteins and characterized their virulence activities and subcellular localizations in the leaf cells of *Arabidopsis thaliana*. Infection assays using bacterial (*Pseudomonas syringae*) and oomycete (*Hyaloperonospora arabidopsidis*) pathogens revealed subsets of candidate effectors that enhanced or decreased pathogen leaf colonization. Confocal imaging of GFP-tagged candidate effectors constitutively expressed in stable transgenic plants revealed that some protein fusions specifically accumulate in nuclei, chloroplasts, plasmodesmata and punctate cytosolic structures. Altogether, our analysis suggests that rust fungal candidate effectors target distinct cellular components in host cells to promote parasitic growth.

Keywords: Fungus, parasite, obligate biotroph, confocal microscopy, virulence assays.

Introduction

Plant-associated organisms secrete effectors that alter the host's cellular structure and functions to promote colonization (Hogenhout *et al.*, 2009). The plethora of plant processes modulated by effectors indicates that effectors target most, if not all, cell structures (Giraldo & Valent, 2013, Petre *et al.*, 2016, Petre *et al.*, 2015b), and that the study of effectors is useful to deepen our understanding of pathogenic processes (Win *et al.*, 2012). Specifically, effectors are used to probe into plant functions that govern plant resistance (i.e. immune response-related pathways) or plant susceptibility (i.e. susceptibility genes). Identifying and manipulating such functions is key to developing resistant crops (Dangl et al., 2013). Using effectors as probes of the plant proteome to pinpoint the precise protein targeted by an effector may identify susceptibility genes in the host. Altering these genes, which are critical for compatibility, could provide durable resistance.

Obligate biotrophic pathogens have to evade and/or suppress host recognition for a lengthy period of time to complete their life cycle whilst their host remains alive. This leads to an intricate battle in which the pathogen rewires the host's cells to meet its needs and to thwart host defenses. Suppression and evasion of innate immunity is undoubtedly an important aspect of obligate biotrophy; it is, however, only a starting point in the establishment of a successful infection. Indeed, it has recently emerged that effectors also target cellular structures and processes that are not directly related to the plant immune system, thus suggesting that pathogens do not only suppress immune responses but also achieve a deep manipulation of their hosts (reviewed in (Chaudhari *et al.*, 2014, Giraldo & Valent, 2013, Win et al., 2012)).

Rust fungi have a complex life cycle, they cannot be cultured *in vitro* and are not easily amenable to transformation, three traits hindering functional investigations. Moreover, these fungi do not infect model plants such as *Arabidopsis thaliana* (Lawrence *et al.*, 2010) and consequently very little is known about the molecular basis of their pathogenicity (Petre *et al.*, 2014). *Melampsora larici-populina* is the causative agent of poplar leaf rust, which has had devastating consequences on poplar plantations worldwide (Duplessis *et al.*, 2009, Feau *et al.*, 2007, Hacquard *et al.*, 2011, Duplessis *et al.*, 2011b). In order to assess the full weaponry at the pathogen's disposal, thorough

genomic information is required. The combination of transcriptome and genome analyses has provided a first glimpse into the putative effector arsenal of *M. larici-populina* (Duplessis *et al.*, 2011a, Hacquard *et al.*, 2010, Hacquard *et al.*, 2012, Joly *et al.*, 2010). Hacquard et al. (2012) identified and annotated 1,184 small secreted proteins that they highlighted as candidate secreted effector proteins (CSEPs). Most of these putative effectors show no sequence similarity to proteins from species outside of Pucciniales and are found in multigene families. A subset of this CSEP repertoire is expressed in haustoria (Hacquard et al., 2012, Hacquard et al., 2010, Joly et al., 2010) and is thus probably enriched in proteins which are effectively delivered inside poplar cells during the infection.

Most of the progress made in effector biology during the last decade relied on heterologous systems enabling the study of effectors in plant cells (Fabro *et al.*, 2011, Sohn *et al.*, 2007, Rafiqi *et al.*, 2012). *Agrobacterium* mediated heterologous expression or *Pseudomonas*-mediated delivery of tagged effectors in leaf cells are methods of choice for studying effectors *in planta* (Torto *et al.*, 2003, Vleeshouwers *et al.*, 2008). Subsequently, confocal imaging of green fluorescent proteins (GFP) fusions is widely used to determine the cellular compartments targeted by effectors (Caillaud *et al.*, 2012, Schornack *et al.*, 2010, Takemoto *et al.*, 2012, Gaouar *et al.*, 2016). More recently, *Nicotiana benthamiana* was used to identify cellular compartments targeted by *M. larici-populina* candidate effectors, as well as putative plant-interacting proteins (Petre et al., 2015b). Effector delivery systems can be coupled with pathogen growth assays to identify effectors possessing virulence activities (Dou *et al.*, 2008, Fabro et al., 2011). However, the use of stable *Arabidopsis* lines has several advantages over transient assays in *N. benthamiana*: it offers the possibility to use well characterized genetic tools such as knock-out lines of putative interactors to search for phenotype similarities; it also enables the assessment of protein localization in guard cells, which are not transformed in transient assays; and it renders possible the generation of stable single insertion homozygous lines which can further be used for crosses, transcriptomic or metabolomic studies.

In this study, we investigated a set of 16 CSEPs of the poplar rust fungus *M. larici-populina* by measuring their ability to promote bacterial and oomycete pathogen

growth in a heterologous system. These CSEPs were stably transformed in *Arabidopsis thaliana* and these lines were used for confocal imaging to assess candidate effectors' subcellular localization *in planta*. Here we demonstrate that CSEPs target various subcellular structures and promote pathogen colonization of leaves.

Results

Selection of 16 *M. larici-populina* CSEPs

We selected 16 CSEPs from a set of 1,184 SSPs previously described (Hacquard et al. 2010, Hacquard et al. 2012) (Table 1). All selected CSEPs were less than 300 amino acids long, had no sequence similarity with proteins from species outside the Pucciniales order, showed induction of transcript expression during poplar leaf infection, and reflected the diversity of CSEPs families in *M. larici-populina*. Among the most informative sources of expression data are a haustoria-specific cDNA library and a transcriptome analysis of laser-microdissected rust-infected poplar leaves (Hacquard et al., 2010, Joly et al., 2010). Several of the selected CSEPs (MLP72983, MLP106078, MLP123218, MLP106078, MLP102036, MLP123531, MLP124305, MLP124518, MLP123531, MLP124305, MLP124466, MLP102036) displayed a very high expression ratio in microdissected palisade mesophyll enriched in haustoria and infection hyphae when compared with microdissected uredinia, mostly composed of spores and sporogenous hyphae (Hacquard et al., 2010). MLP124497, MLP124499 and MLP124518 [Mlp0032_0018] are different members of the same CSEP family, which was previously designated CPGH1 (Hacquard et al., 2012). This family of very small proteins (<100 amino acids) presents signatures of positive selection and is over-represented in the haustorial library (Hacquard et al., 2012, Joly et al., 2010). MLP37347 was selected for its homology to AvrL567, a previously reported effector of the flax rust fungus *Melampsora lini* (Dodds et al., 2004). MLP123227 (SSP15), shows a bimodal expression profile *in planta* and immunolocalization data indicates it has an intriguing localization pattern *in planta*, both in haustoria and sporogenous hyphae (Hacquard et. 2012). The last two CSEPs (MLP123437 and MLP124111) belong to different classes of SSPs conserved in *Puccinia* spp. (classes VI and III; Hacquard et al., 2012) and they display a conserved

exon/intron structure and a characteristic spacing of Cys residues (including the presence of Y/FxC motifs) (Hacquard et al., 2012).

Three CSEPs promote the growth of *P. syringae in planta* independently of PTI suppression

To test whether the 16 CSEPs can promote pathogen growth, we performed infection assays using the *P. syringae* pv. *tomato* DC3000/*A. thaliana* pathosystem (Sohn et al., 2007). In this system, the sequences coding for the mature form of the CSEP, i.e. without the predicted signal peptide, are fused to the N-terminus of AvrRPM1 to drive their translocation inside host cells via the type three secretion apparatus of *P. syringae*. Five out of sixteen CSEPs significantly increased bacterial growth *in planta* (MLP124499, MLP102036, MLP124266, MLP124497, MLP106078) (Figure 1A). Conversely, two candidate effectors decreased bacterial growth (MLP123227, MLP37347), while the other nine did not affect bacterial growth when compared to the control. Standard growth assays confirmed that the CSEPs did not affect the rate of bacterial cell division (data not shown), thus suggesting that alteration of *in planta* bacterial growth is caused by the effect of the CSEP on plant cells. We conclude that five CSEPs promote the growth of *P. syringae* when delivered by the bacteria, suggesting that they have a virulence activity in leaf cells.

To complement the effector delivery assays, we generated stable *A. thaliana* transgenic lines constitutively expressing CSEP-GFP fusions. Transgenic lines were generated for 14 CSEPs, while lines MLP124111 and MLP123437 could not be retrieved. Then we performed infection assays using wild-type *P. syringae* pv *tomato* DC3000 on the aforementioned transgenic lines. Five of the fourteen CSEPs promoted the bacterial growth (MLP123218, MLP124466, MLP124497, MLP124499 and MLP106078), while two (MLP37347 and MLP123227) showed less growth compared to the control plants (Figure 1B). The combined results from these two experiments indicate that three CSEPs (MLP124499, MLP124497, MLP106078) promoted bacterial growth while two (MLP37347 and MLP123227) reduced bacterial growth in both assays.

In order to understand how these CSEPs (MLP123218, MLP124466, MLP124266, MLP124497 and MLP106078) contribute to bacterial growth increase, we

selected the transgenic lines that displayed increased bacterial growth and infected them with the type III secretion-deficient bacterial strain *P. syringae* pv. DC3000 *hrcC-*. Although this strain is unable to produce a functional T3SS and inject effectors in host cells, it still carries pathogen associate molecular patterns that will initiate PTI. Therefore, we monitored bacterial growth at day 0 and day 3 in transgenic lines, Col-0 and a transgenic line expressing GFP without any effector (control). The results shown in Figure 1C demonstrate that *P. syringae* pv. DC3000 *hrcC-* growth is not affected by the effectors when compared to the control. Taken together these results suggest that PTI is not suppressed by the effectors that contribute to increased bacterial growth.

Eleven CSEPs promote the growth of *Hyaloperonospora arabidopsidis in planta*

Since *M. larici-populina* is an obligate biotrophic filamentous pathogen, we sought to test whether the CSEPs would affect the growth of a pathogen with a similar lifestyle. Since no rust infect *A. thaliana*, we used the oomycete *Hyaloperonospora arabidopsidis* to challenge the transgenic plants constitutively expressing the candidate effectors. In total, 11 out of 14 transgenic lines expressing CSEPs supported more *H. arabidopsidis* sporulation than control plants (mean ratio of two, 15,000 to 25,000 vs 10,000 spores/g of leaf tissue) (Figure 2). However, no CSEP-GFP line promoted the growth of *H. arabidopsidis* at a comparable level to the infection control line *eds1,* which is hypersensitive to *H. arabidopsidis*. We conclude that the majority (> 75%) of the tested CSEPs promote *H. arabidopsidis* growth on *A. thaliana*.

Only two CSEPs (MLP124497, MLP124499) promote pathogen growth in the three infection assays

In order to evaluate the consistency of the virulence activities detected for the CSEPs, we compared the results from the three sets of infection assays. This analysis revealed that all CSEPs promoted pathogen growth in at least one experiment, three did so in the two experiments involving *P. syringae*, while only two (MLP124497, MLP124499) promoted pathogen growth in all three experiments (Figures 1, 2, 3). Conversely, while two candidate effectors consistently reduced the growth of *P. syringae* in both *in planta* experiments, they did not affect *H. arabidopsidis* growth. Some

candidate effectors did not alter bacterial growth (MLP124256, MLP124518, MLP124266, MLP123531, MLP124305, MLP72983), but did significantly promote *H. arabidopsidis* growth *in planta* (Figures 1, 2 and 3). Interestingly, the CSEP that promoted the highest bacterial growth (MLP106078) did not significantly enhance *H. arabidopsidis* growth. Based on these results we conclude that MLP124497 and MLP124499 promote the growth of unrelated pathogens in *A. thaliana*, while other CSEPs exhibit a pathogen-specific growth-promoting effect.

The transgenic line 124499 shows delayed senescence

We assessed the phenotypes of the transgenic lines to see if they displayed any growth or morphological alteration that could be caused by the expression of the fungal genes. To this end, the plants were grown at 20º C as well as at 16º C and senescence was monitored as they aged. Supplementary figures 1 and 2 show representative plants from each transgenic line when grown at 20 ºC (Supplementary figure 1) and 16 ºC (Supplementary figure 2). Most lines did not show any striking phenotype, except MLP124499 plants, whose leaves remained green much longer than all other transgenic and Col-0 plants. To ensure that this was not a positional effect in the flat, we started a new flat with alternating rows of Col-0 and MLP124499 plants (Supplementary figure 3; tagged as H1) and we again observed that the rows of MLP124499 remained green while the Col-0 plant had completely dried. We concluded that, except for the transgenic line MLP124499, the phenotype of the CSEPs expressing plants was unaffected.

Three candidate effectors specifically accumulate in chloroplasts, cytosolic bodies, and at plasmodesmata

To gain further insight into the growth-promoting effect of CSEPs, we used confocal microscopy to determine the subcellular localization of the CSEP-GFP fusions in leaf epidermal cells (i.e. guard and pavement cells) obtained from the *A. thaliana* stable transgenic lines. Three candidate effectors specifically accumulated in chloroplasts (MLP72983) and cytosolic puncta (MLP37347, MLP124305) (Figure 4A). The fluorescence signal of MLP72983 was distributed homogenously within the chloroplasts, suggesting that it accumulates in the stroma. The fluorescence signal of MLP37347 was

restricted to small, bright, and circular cytosolic structures of approximately 1 µm in diameter and of unknown nature, whereas the fluorescence signal of MLP124305 accumulated in small cytosolic dots that were excluded from nuclei (Figure 4A). In order to investigate the nature of these cytosolic foci we performed co-localisation experiments of MLP37347 and MLP124305 with PDCB1-mCherry, a plasmodesmata marker, and RBP47b-CFP, a stress granule marker. MLP37347-GFP and PDCB1-mCherry fluorescent signals overlapped in punctate structures, indicating that this CSEP accumulates at the plasmodesmata (Figure 4B). MLP124305 neither localized to the plasmodesmata nor the stress granules (not shown). To find the true localization of MLP124305-GFP we crossed the transgenic line overexpressing MLP124305-GFP with DCP1-CFP (a processing body marker) but did not observe co-localization, therefore we do not know what the structure targeted by this effector is. The eleven remaining CSEPs showed a non-informative distribution in the cytosol and in the nucleus, similar to the free GFP control (Figure 4A). Anti-GFP western blots revealed a single band signal at the expected size for all but one CSEP-GFP, suggesting that the fusions were neither cleaved nor modified in leaf cells (Supplementary figure 4). MLP124305 yielded multiple bands of lower molecular weight, suggesting protein degradation (data not shown). We conclude that out of the sixteen CSEPs, three target specific cellular structures in leaf cells: some undefined cytosolic puncta, the chloroplast and plasmodesmata.

Discussion

In this study, we used *A. thaliana* as a heterologous system to perform the functional analysis of a subset of 16 candidate secreted effector proteins (CSEPs) from the poplar leaf rust fungus *Melampsora larici-populina*. Notably, we identified several CSEPs that promote bacterial or oomycete pathogen growth *in planta*, as well as some that accumulate in distinct plant cell compartments. These proteins were flagged as putative virulence factors that needed to be investigated further.

Functional studies of rust fungi are challenging due to the obligate biotrophic status of these pathogens, and high throughput 'effectoromics' approaches are needed (Petre et al., 2014, Petre *et al.*, 2015a, Petre et al., 2015b). Such procedures are not fully available yet in most rust pathosystems. We sought to partially fulfill this need by using

heterologous systems, a strategy increasingly used in rust effector biology (Petre et al., 2015a, Petre et al., 2016, Petre et al., 2015b). To this end, we created a collection of *A. thaliana* transgenic lines to investigate the subcellular localization and virulence activities of rust CSEPs, complementing the efforts accomplished thus far using *N. benthamiana* as a heterologous system. These lines represent a valuable resource for the community. For instance, they could be used in proteomic approaches to find interaction partners, confirming co-immunoprecipitation results from *N. benthamiana* and/or to study the impact of effectors on the plant transcriptome and metabolome.

Ideally, the confirmation that a small secreted protein is a *bona fide* effector requires the demonstration that it has the capacity to interfere with a host component to ultimately favor pathogenesis. Hence we used pathogen growth as a proxy to measure the effect of these CSEPs on host cells. Three out of the sixteen candidate effectors tested (18%) robustly enhanced bacterial growth *in planta*. In contrast, when using a similar experimental set-up, Fabro et al. (2011) showed that 70% of *Hpa* candidate effectors set caused an increase in bacterial growth. There are two possibilities that may explain the difference of number between this study and our results. First, our assays were performed in a non-host plant, in which *M. larici-populina* CSEPs might not be functional; second, Fabro et al. (2011) used RxLR candidate effectors that are all likely to be host-translocated, while our portfolio may have included apoplastic candidate effectors or even non-effectors that are predicted secreted proteins and remain in the apoplastic space of the native poplar-poplar rust pathosystem.

Bacterial infection assays revealed dissimilarities depending on whether CSEPs were bacteria delivered or constitutively expressed *in planta*. For example, MLP123218 and MLP124466 had a positive effect on pathogen growth when expressed *in planta*, but none when they were bacterially delivered. Conversely, MLP102036 and MLP124266 had a positive effect on pathogen growth when they were bacterially delivered, but none when they were constitutively expressed. Two factors may explain the differences. First, bacterially produced CSEPs may be mistargeted or misfolded due to their passage through the T3SS to reach the plant cell. Second, GFP tags may generate steric interference causing a mistargeting or misfolding of the CSEPs, especially if they are small.

The demonstrated function of many effectors is to suppress PTI (Gohre & Robatzek, 2008, Zhang *et al.*, 2007). To study this possibility, we used the *P. syringae* pv *tomato* DC3000 *hrcC*- strain, which is deficient in the production of the type III secretion system and which triggers PTI but not ETI. Our infection results with bacteria and oomycete suggested that the increased pathogen growth observed with MLP106078, MLP124497 and MLP124499 were not caused by PTI suppression. Remarkably, it suggests that the CSEPs assayed favor pathogen infection without suppressing plant immunity. Other aspects of the plant immunity, such as ROS production and signaling pathways, are currently being investigated as part of a more detailed analysis of these CSEPs. Since obligate biotrophs are extremely sophisticated parasites that often establish long-standing associations with host tissues, we speculate that many of their effectors not only suppress immune responses like many hemi-biotrophs do, but deeply modulate host functions.

Our results show that infection assays using different pathogens having various lifestyles, i.e. bacteria and oomycete, can yield strikingly different results. *Hpa* and *M. larici-populina* are both obligate biotrophic filamentous pathogens of dicot plants and they share some similarities in their propagation mode in leaf tissues. Therefore, one would expect that *Hpa* pathogenicity would be more likely to be affected by rust effectors than *P. syringae* bacterial pathogenicity. Indeed, our results showed that 11 CSEPs promoted the growth of *Hpa*, which is more than twice the number of CSEPs promoting the growth of *P. syringae*. It is possible that *M. larici-populina* CSEPs target mechanisms that specifically assist in leaf infection by biotrophic pathogens.

We could identify rust CSEPs affecting pathogen growth in *A. thaliana*, a non- host plant. Since many effectors exert their activities by associating with plant proteins, this observation suggests that some CSEPs may have the ability to associate with *A. thaliana* proteins despite the fact that they do not under natural conditions. In line with this hypothesis, Petre et al. (2015, 2016) identified rust CSEPs that associate with specific *N. benthamiana* proteins which have conserved homologs in the natural host plants poplar. Since our present report includes candidate effectors that were also investigated by Petre et al. (2015), we assessed whether some of the putative targets identified by co-

immunoprecipitation/mass spectrometry could explain the pathogen assays results that we observed. Only two effectors common between the two studies had specific interactors, MLP37347 and MLP124111. MLP124111 did not show any effect on pathogen growth when the effector was delivered by *P. syringae* and could unfortunately not be assayed with the effector constitutively expressed *in planta* as it did not produce a viable transgenic line. MLP37347 on the other hand displayed an interesting effect: it decreased bacterial growth (in both systems) but increased oomycete growth. In the co-immunoprecipitation assay, MLP37347 had a single specific interactor, which is the glutamate decarboxylase 1 (GAD1). It should be noted that MLP37347 is the effector localized to the plasmodesmata. Evaluation of the potential role of the glutamate decarboxylase 1 as a putative virulence target of MLP37347 will require further investigation.

Two CSEPs (MLP37347, MLP123227) had a negative effect on bacterial growth but a positive effect on *H. arabidopsidis* growth. One option for that decreased bacterial growth is their possible recognition by *A. thaliana*'s immune receptors and the triggering of the defense responses. *M. larici-populina* is non-host on Arabidopsis nor is any rust fungus, and for this reason it seems surprising that *A. thaliana* would recognize these candidate effectors. We rather hypothesize that *Arabidopsis* does not directly recognize those CSEPs; but that instead they may target proteins guarded by a R-protein in *A. thaliana* (Dangl & Jones, 2001, Van der Biezen & Jones, 1998). Thus, the identification of the target of these CSEPs could provide information with regards to decoy or bait, and ultimately, by homology, allow the identification of important components of the plant immune system (Khan *et al.*, 2016). We also have to keep in mind that the expression of a given effector in *P. syringae* may affect the secretion of other of its endogenous effectors and may thus decrease its virulence.

Confocal microscopy assays revealed that some candidate effectors accumulated in chloroplasts, plasmodesmata and cytosolic foci in leaf cells, while most displayed non-informative nucleocytosolic distribution. It is important to consider that these localizations were obtained using expression driven by the 35S promoter, so it could be different from what would be observed when the CSEPs are delivered by the pathogen. Petre et al. (2015a) studied the localization and interaction partners of some *M. larici-*

populina CSEPs. In both studies, the subcellular localization of MLP102036, MLP123227, MLP124266, MLP124497, MLP124499 and MLP37347 was identical. Interestingly, several rust candidate effectors accumulate in chloroplasts (Petre et al., 2015a, 2015b, 2016). Despite intensive cell biology screens, no other effectors of filamentous pathogens were reported to target chloroplasts. Whether chloroplasts are important organelles for rust fungi to manipulate remains to be investigated. The similar localization of the common CSEPs in both studies strengthens the use of heterologous systems to infer CSEPs localization, putative function and interaction partner studies.

We could not recover stable transgenic lines expressing MLP124111 and MLP123437, which suggests that their accumulation in cells could be toxic to plants. MLP123437 was not investigated by Petre et al. 2015, however using *N. benthamiana* Mlp124111 localized in chloroplasts as well as in large, bright, and irregular cytosolic structures that were probably aggregates. It is possible that these aggregates, as they may be toxic to the cell, were the reason why a stable transgenic line for MLP124111 could not be recovered, although no sign of necrosis was reported by Petre et al. (2015). Alternatively, chloroplastic localization could trigger the chlorosis we observed in the unique transgenic T1 line obtained which never reached maturity. Our results demonstrate that advances in rust fungi biology, as well as in the biology of other obligate biotrophs that cannot be easily and/or routinely transformed, rely on the combination of parallel approaches (e.g. *in vitro* and heterologous assays). Our approach is much valuable due to the large pool of genetic knowledge and resources that are available for *Arabidopsis* compared to *Nicotiana*.

Material and methods

Plasmid constructs

DNA sequences encoding all mature small secreted proteins were ordered from GenScript in a lyophilized form (the stop codon was removed to enable GFP fusion). All constructs were transferred by BP recombination to the Gateway pDONR Zeo vector (Invitrogen, Carlsbad, CA, USA). From pDONR™/Zeo, contructs were either sent to pB7FWG2 (Karimi *et al.*, 2002) to generate stable C-terminally GFP-tagged transgenic Arabidopsis plants or pVSP-PsSPdes (courtesy of Guus Bakkeren's laboratory) for *Pseudomonas* infection assays. pVSP-PsSPdes harbors the AvrRPM1 secretion signal and a C-terminal HA tag (Rentel *et al.*, 2008).

Transformation of *A. thaliana*, pathogen assay and western blotting

Five week old soil-grown *Arabidopsis thaliana* plants were transformed using the floral dip method with minor modification (Clough & Bent, 1998). Modifications included substituting Silwet L-77 by OFX-0309 (Norac Concept Inc, Guelph, ON, Canada) (Mireault *et al.*, 2014) and dipping the plants a second time one week later to increase the number of transformants. T1 plants were selected using ammonium glufosinate (Basta) at 60 mg/L. T2 plants grown in Petri dishes (with Basta at 25 mg/L), and lines displaying a 3:1 ratio were selected to obtained single insertion lines. T3 plants were also grown in Petri dishes, and lines showing 100% germination were selected as homozygotes. An average of twelve transgenic lines for each construct were selected and screened for GFP expression by Western blot (Supplementary Figure 1), and the strongest expressing line was kept for each construct. This primary screen was necessary to ensure that the GFP was not being cleaved from the small secreted proteins in which case we would have observed fluorescence signal from a free GFP in confocal microscopy. It should also be noted that two constructs did not yield any transgenic lines despite many transformation attempts; these are SSPs MLP124111 and MLP123437. In fact, one line was recovered from MLP124111 but it showed important chlorosis, stunted morphology, it did not grow higher than 2 cm in seven weeks, it never produced any viable seeds and died. Additional attempts to produce more transgenic lines overexpressing MLP124111 failed. We conclude that constitutive *in planta* expression of MLP124111 and perhaps MLP123437 is most likely toxic to the plant. Infections were carried out on one line per construct.

Western blots and infection assays were performed as previously described (Germain *et al.*, 2010, Germain *et al.*, 2007). Briefly, bacterial infections were performed with four week-old Arabidopsis plants grown at 22ºC in a 16/8h light/dark cycle. *Ps* pv. *tomato* diluted at OD_{600} 0.001 were leaf-inoculated on the abaxial side of the leaf. A minimum of 36 leaves were infected for each effector or transgenic line. Leaf punches were taken from 12 leaves at day 0 and 24 were taken at day 3 to assess bacterial quantity. *Hpa* infection were performed as described in Dong et al. 2016 with no modification to the protocol (Dong *et al.*, 2016). For Western blots, two leaf punches (0.384 cm^2) were taken from 3-weeks-old T3 plants and stored at -80ºC. Leaf punches were disrupted using a TissueLyser (Qiagen, Toronto, ON, Canada) and a 5 mm stainless steel bead agitated at 26 cycles/sec for 10 sec. Laemli sample buffer (100µL) was added and the tube was heated at 95ºC for 5 min and spun at 13,000 g for 1 min. Supernatant (10µL) was loaded on a 10% acrylamide gel. Western blot was carried out as previously described (Germain et al., 2007); the mouse anti-GFP antibody used to detect the recombinant protein was purchased from Cedarlane (Burlington, ON, Canada) and used at 1:5000.

Confocal imaging

T3 seedlings 6-10 days' old collected from Petri dishes containing ½ MS media + ammonium glufosinate (25 mg/L) were placed in a water drop under a cover slip and imaged immediately. Before each imaging session, wild-type plants were visualized to adjust the settings in order to exclude the autofluorescence of the chloroplasts. Images were captured with a Carl Zeiss LSM700 or Nikon A1 confocal microscope. 40X oil PlanApo immersion objectives were used. Excitation laser (488 nm) was used and photons were collected between 510 and 520 nm. Image analysis was performed with ImageJ (http://imagej.nih.gov/ij/).

Acknowledgments

We are thankful to Carl Zeiss Corporation and Nikon Instruments for giving us the opportunities to freely use the Zeiss 410 and Nikon A1 confocal microscope respectively. We also thank Isabelle Lamarre and Franck Stefani (Laurentian Forestry Centre) for editorial work. HG's and DLJ' post-doctoral fellowships were supported by the Natural

Sciences and Engineering Research Council of Canada (NSERC). Funding for the project was also provided by NSERC Discovery Grants to HG and AS. The project in HG's laboratory was also partially funded by an institutional research chair held by HG. CM received an undergraduate student award from NSERC. BP was supported by an INRA Contrat Jeune Scientifique, by the European Union, (as part of the Marie-Curie FP7 COFUND People Programme, through an AgreenSkills' fellowship (under grant agreement no. 267196), and by the Laboratory of Excellence ARBRE, through a mobility grant (12RW53). SD is supported by the French National Research Agency through the Laboratory of Excellence ARBRE (ANR-12-LABXARBRE-01) and the Young Scientist Grant POPRUST (ANR-2010-JCJC-1709-01). We are grateful to Jean-François Laliberté (INRS Armand-Frappier, Qc Canada) for providing the plasmodesmata marker pDCB1-mCherry. We also thank professor Dan Robert for providing the RBP47CFP construct.

Figure legends

Figure 1. Bacterial growth *in planta* differs when effectors are delivered by bacteria or are constitutively expressed

A) Growth of *Pst* DC3000 without (EV) or with candidate effectors (all other lanes) was measured on the day of infection and 3 days after infection of 4-week-old plants by leaf infiltration. A bacterial suspension of OD_{600} = 0.001 was used as inoculum. Statistical significance was evaluated using Student's t-test ($p<0.05$); asterisks indicate statistically significant differences between the effector and empty vector. The experiment was repeated at least three times (a representative experiment is shown).

B) Growth of *Pst* DC3000 wild-type infecting plants expressing an effector, Col-0 or Col-0 expressing GFP was measured on the day of infection and 3 days after infection of 4-week-old plants by leaf infiltration. A bacterial suspension of OD_{600} = 0.001 was used as inoculum. Statistical significance was evaluated using Student's t-test ($p<0.05$); asterisk indicates statistically significant difference between plants carrying effector and Col-0 expressing GFP. Five replicates were included for each genotype. To facilitate the comparison with Figure 1A, each transgenic line is presented in the same order. The experiment was repeated at least three times (a representative experiment is shown).

C) Growth of *Pst* DC3000 hrcC- strain infecting plants expressing an effector, Col-0 or Col-0 expressing GFP was measured on the day of infection and 3 days after infection of 4-week-old plants by leaf infiltration. A bacterial suspension of OD_{600} = 0.001 was used as inoculum. Statistical significance was evaluated using Student's t-test ($p<0.05$); asterisk indicates statistically significant difference between plants carrying effector and Col-0 expressing GFP. Five replicates were included for each genotype. The experiment was repeated at least three times (a representative experiment is shown). Note that no transgenic lines were recovered for 123437 and 124111.

Figure 2. Most candidates effector affect the growth of *H.arabidopsidis* Noco2 **when constitutively expressed *in planta*.**

Two week-old soil-grown plants were inoculated with *H. arabidopsidis* Noco2 at a concentration of 20,000 conidiospores per ml and the number of conidiospores was quantified 7 days after inoculation. Bars represent the mean of four replicates. Statistical significance was established using Student's t-test ($p<0.05$), and statistically significant differences are represented by an asterisk between plants carrying effector and Col-0 expressing GFP. Each transgenic line is ordered as in Figure 1 for easier comparison. The experiment was repeated five times (representative experiment is shown).

Figure 3. Venn diagram showing the candidate effectors that induced increased virulence (in black) or decreased virulence (in red) .

Note that no transgenic lines were recovered for 123437 and 124111.

Figure 4. Subcellular localization of the different candidate effectors.

A) Confocal images of leaf epidermal cells of 7 day old transgenic plantlets expressing candidate effectors fused to GFP (SSP-GFP) in Col-0 genetic background. The top three effectors are the ones displaying informative localization, while the bottom three rows display the effectors showing nucleocytoplasmic localization.

B) Colocalization between PDCB1-mCherry , a plasmodesmata marker and 37347-GFP to infer its localization. Left panel red channel, center panel green channel, right panel overlay with DIC.

Supplementary Figure 1. Pictures of plant after 4 weeks of growth at 20ºC.

Supplementary Figure 2. Pictures of plant after 4 weeks of growth at 16ºC.

Supplementary Figure 3. Pictures of 124499 and Col-0 plants after 6 weeks of growth at 20ºC to vizualize senescence.

Supplementary Figure 4. Western blot showing the molecular weight of the different candidate effectors tagged with the GFP protein

Immunoblot analysis performed using an anti-GFP antibody. Molecular weight was calculated using the BioRad Low molecular weight protein standard. Only the transgenic line that was selected for infection and confocal imaging is shown.

Supplementary Table 1.

Full DNA and peptide sequences of the candidate effectors. --- indicates where the candidate effector is predicted to be cleaved. The C-terminal section was used as the mature protein.

Table 1.

ProteinID[a]	CPG or Class (number of members)[b]	Protein (signal peptide) length[c]	Cysteine residues[d]	Evidence of expression[e]	Signature of positive selection[f]	Homology to *M. lini* HESPs[g]	Homology in *Pgt*[g]	Effect on pathogen growth[h]	Sub-cellular localisation
37347	-	152 (23)	2	OA	-	AvrL567	-	-, -, +	Plasmodesmata
72983	CPG332-CPG333 (13)	220 (26)	8	S, I, H, OA, A3	-	-	Yes	N, N, +	Chloroplast
102036	CPG2528 (5)	107 (25)	0	H, OA, A3	-	-	-	+, N, N	Nucleocytoplasmic
106078	-	137 (21)	10	I, OA, A3	-	-	-	+, +, N	Nucleocytoplasmic
123218	CPG543 (7)	209 (19)	6	I, OA, A3	-	-	Yes	N, +, +	Nucleocytoplasmic
123227 (SSP15)	CPG1059 (2)	124 (24)	3	I, OA	-	-	-	-, -, +	Nucleocytoplasmic
123437	Class VI (6)	180 (20)	11	I, H, OA	-	HESP-C49	Yes	N	Not available
123531	CPG4557 (2)	102 (21)	8	I, OA, A3	-	-	-	N, N, +	Nucleocytoplasmic
124111	Class III (8)	135 (21)	10	H	-	-	Yes	N	Not available
124256	CPG5464 (13)	89 (25)	6	I	Yes	AvrP4	-	N, N, +	Nucleocytoplasmic
124266	CPG5464 (13)	92 (25)	7	I, H	Yes	AvrP4	-	+, N, +	Nucleocytoplasmic
124305	CPG5184 (2)	147 (25)	12	OA, A3	-	-	-	N, N, +	Cytoplasmic foci
124466	-	76 (24)	0	H, OA, A3	-	-	-	N, +, N	Nucleocytoplasmic
124497	CPGH1 (33)	77 (21)	4	I, H, OA	Yes	-	-	+, +, +	Nucleocytoplasmic
124499	CPGH1 (33)	72 (21)	3	I, H	Yes	-	-	+. +, +	Nucleocytoplasmic
124518	CPGH1 (33)	76 (21)	3	I, H, OA, A3	Yes	-	-	N, N, +	Nucleocytoplasmic

[a] Best predicted gene model in the *M. larici-populina* isolate 98AG31 JGI genome sequence.

[b] Families, clusters of paralogous genes (CPGs) and classes of small-secreted proteins as described in Duplessis et al., 2011 and Hacquard et al., 2012. Number between brackets indicate the number of members in gene families.

[c] Numbers of amino acids are indicated.

[d] Number of cysteine residues in the mature form of the protein (i.e. without signal peptide)

[e]Evidence of expression among S (Expressed Sequence Tags from resting spores, (Duplessis et al., 2011a), I (Roche 454 data from infected leaves, (Hacquard et al., 2012), H (Expressed Sequence Tags from isolated haustoria, (Joly et al., 2010), OA (oligoarray data from infected leaves, (Duplessis et al., 2011a), A3 (most highly upregulated transcripts from oligoarray data in the palisade mesophyll versus sporogenous microdissected structures, (Hacquard et al., 2010).

[f] As described in Hacquard et al., (2012).

[g] Homology searches were carried out against UNIPROT and *Puccinia* Group Database using blastp (*E* value <1e-6). Pgt = *Puccinia graminis* f. sp. *tritici*.

[h]First position indicate effect on bacterial growth when the effector is delivered by *Pst*, second position denote effect on bacterial growth when the effector is expressed *in planta*, third position denote effect on *Hpa* growth when the effector is expressed *in planta*. + =positive effect, N= no effect, - = negative effect.

Bibliography

Caillaud, M. C., Piquerez, S. J., Fabro, G., Steinbrenner, J., Ishaque, N., Beynon, J.*, et al.* (2012) Subcellular localization of the Hpa RxLR effector repertoire identifies a tonoplast-associated protein HaRxL17 that confers enhanced plant susceptibility. *The Plant journal : for cell and molecular biology,* **69,** 252-265.

Chaudhari, P., Ahmed, B., Joly, D. L. and Germain, H. (2014) Effector biology during biotrophic invasion of plant cells. *Virulence,* **5,** 1-7.

Clough, S. J. and Bent, A. F. (1998) Floral dip: a simplified method for *Agrobacterium*-mediated transformation of *Arabidopsis thaliana*. *The Plant Journal,* **16,** 735-743.

Dangl, J. L. and Jones, J. D. G. (2001) Plant pathogens and integrated defence responses to infection. *Nature,* **411,** 826-833.

Dodds, P. N., Lawrence, G. J., Catanzariti, A. M., Ayliffe, M. A. and Ellis, J. G. (2004) The Melampsora lini AvrL567 avirulence genes are expressed in haustoria and their products are recognized inside plant cells. *The Plant cell,* **16,** 755-768.

Dong, O. X., Meteignier, L. V., Plourde, M. B., Ahmed, B., Wang, M., Jensen, C.*, et al.* (2016) Arabidopsis TAF15b Localizes to RNA Processing Bodies and Contributes to snc1-Mediated Autoimmunity. *Molecular plant-microbe interactions : MPMI***,** MPMI11150246R.

Dou, D., Kale, S. D., Wang, X., Chen, Y., Wang, Q., Wang, X.*, et al.* (2008) Conserved C-terminal motifs required for avirulence and suppression of cell death by *Phytophthora sojae* effector Avr1b. *The Plant cell,* **20,** 1118-1133.

Duplessis, S., Cuomo, C. A., Lin, Y. C., Aerts, A., Tisserant, E., Veneault-Fourrey, C.*, et al.* (2011a) Obligate biotrophy features unraveled by the genomic analysis of rust fungi. *Proceedings of the National Academy of Sciences of the United States of America,* **108,** 9166-9171.

Duplessis, S., Joly, D. L. and Dodds, P. N. (2011b) Rust Effectors. In: *Effectors in Plant–Microbe Interactions.* Wiley-Blackwell, pp. 155-193.

Duplessis, S., Major, I., Martin, F. and Séguin, A. (2009) Poplar and Pathogen Interactions: Insights from Populus Genome-Wide Analyses of Resistance and Defense Gene Families and Gene Expression Profiling. *Critical Reviews in Plant Sciences,* **28,** 309-334.

Fabro, G., Steinbrenner, J., Coates, M., Ishaque, N., Baxter, L., Studholme, D. J.*, et al.* (2011) Multiple candidate effectors from the oomycete pathogen *Hyaloperonospora arabidopsidis* suppress host plant immunity. *PLoS Pathogen,* **7,** e1002348.

Feau, N., Joly, D. L. and Hamelin, R. C. (2007) Poplar leaf rusts: model pathogens for a model treeThis minireview is one of a selection of papers published in the Special Issue on Poplar Research in Canada. *Canadian Journal of Botany,* **85,** 1127-1135.

Gaouar, O., Morency, M.-J., Letanneur, C., Séguin, A. and Germain, H. (2016) The 124202 candidate effector of Melampsora larici-populina interacts with membranes in Nicotiana and Arabidopsis. *Canadian Journal of Plant Pathology***,** null-null.

Germain, H., Houde, J., Gray-Mitsumune, M., Sawasaki, T., Endo, Y., Rivoal, J.*, et al.* (2007) Characterization of ScORK28, a transmembrane functional protein receptor kinase predominantly expressed in ovaries from the wild potato species *Solanum chacoense*. *FEBS Letters,* **581,** 5137-5142.

Germain, H., Qu, N., Cheng, Y. T., Lee, E., Huang, Y., Dong, O. X.*, et al.* (2010) MOS11: a new component in the mRNA export pathway. *PLoS Genetics,* **6,** e1001250.

Giraldo, M. C. and Valent, B. (2013) Filamentous plant pathogen effectors in action. *Nature reviews. Microbiology,* **11,** 800-814.

Gohre, V. and Robatzek, S. (2008) Breaking the barriers: microbial effector molecules subvert plant immunity. *Annual review of phytopathology,* **46,** 189-215.

Hacquard, S., Delaruelle, C., Legue, V., Tisserant, E., Kohler, A., Frey, P.*, et al.* (2010) Laser capture microdissection of uredinia formed by *Melampsora larici-populina* revealed a transcriptional switch between biotrophy and sporulation. *Molecular plant-microbe interactions,* **23,** 1275-1286.

Hacquard, S., Joly, D. L., Lin, Y. C., Tisserant, E., Feau, N., Delaruelle, C.*, et al.* (2012) A comprehensive analysis of genes encoding small secreted proteins identifies candidate effectors in *Melampsora larici-populina* (poplar leaf rust). *Molecular plant-microbe interactions,* **25,** 279-293.

Hacquard, S., Petre, B., Frey, P., Hecker, A., Rouhier, N. and Duplessis, S. (2011) The poplar-poplar rust interaction: insights from genomics and transcriptomics. *Journal of pathogens,* **2011,** 716041.

Hogenhout, S. A., Van der Hoorn, R. A., Terauchi, R. and Kamoun, S. (2009) Emerging concepts in effector biology of plant-associated organisms. *Molecular plant-microbe interactions : MPMI,* **22,** 115-122.

Joly, D. L., Feau, N., Tanguay, P. and Hamelin, R. C. (2010) Comparative analysis of secreted protein evolution using expressed sequence tags from four poplar leaf rusts (Melampsora spp.). *BMC genomics,* **11,** 422.

Karimi, M., Inze, D. and Depicker, A. (2002) GATEWAY vectors for *Agrobacterium*-mediated plant transformation. *Trends in plant science,* **7,** 193-195.

Khan, M., Subramaniam, R. and Desveaux, D. (2016) Of guards, decoys, baits and traps: pathogen perception in plants by type III effector sensors. *Current opinion in microbiology,* **29,** 49-55.

Lawrence, G. J., Dodds, P. N. and Ellis, J. G. (2010) Transformation of the flax rust fungus, *Melampsora lini*: selection via silencing of an avirulence gene. *The Plant journal : for cell and molecular biology,* **61,** 364-369.

Mireault, C., Paris, L.-E. and Germain, H. (2014) Enhancement of the Arabidopsis floral dip method with XIAMETER OFX-0309 as alternative to Silwet L-77 surfactant. *Botany,* **92,** 1-3.

Petre, B., Joly, D. L. and Duplessis, S. (2014) Effector proteins of rust fungi. *Frontiers in plant science,* **55,** 416.

Petre, B., Lorrain, C., Saunders, D. G. O., Win, J., Sklenar, J., Duplessis, S.*, et al.* (2015a) Rust fungal effectors mimic host transit peptides to translocate into chloroplasts. *Cellular Microbiology***,** n/a-n/a.

Petre, B., Saunders, D. G., Sklenar, J., Lorrain, C., Krasileva, K. V., Win, J.*, et al.* (2016) Heterologous Expression Screens in Nicotiana benthamiana Identify a Candidate Effector of the Wheat Yellow Rust Pathogen that Associates with Processing Bodies. *PloS one,* **11,** e0149035.

Petre, B., Saunders, D. G., Sklenar, J., Lorrain, C., Win, J., Duplessis, S.*, et al.* (2015b) Candidate Effector Proteins of the Rust Pathogen Melampsora larici-populina Target Diverse Plant Cell Compartments. *Molecular plant-microbe interactions : MPMI,* **28,** 689-700.

Rafiqi, M., Ellis, J. G., Ludowici, V. A., Hardham, A. R. and Dodds, P. N. (2012) Challenges and progress towards understanding the role of effectors in plant-fungal interactions. *Current opinion in plant biology,* **15,** 477-482.

Rentel, M. C., Leonelli, L., Dahlbeck, D., Zhao, B. and Staskawicz, B. J. (2008) Recognition of the Hyaloperonospora parasitica effector ATR13 triggers resistance against oomycete, bacterial, and viral pathogens. *Proceedings of the National Academy of Sciences of the United States of America,* **105,** 1091-1096.

Schornack, S., van Damme, M., Bozkurt, T. O., Cano, L. M., Smoker, M., Thines, M*., et al.* (2010) Ancient class of translocated oomycete effectors targets the host nucleus. *Proceedings of the National Academy of Sciences of the United States of America,* **107,** 17421-17426.

Sohn, K. H., Lei, R., Nemri, A. and Jones, J. D. (2007) The downy mildew effector proteins ATR1 and ATR13 promote disease susceptibility in *Arabidopsis thaliana*. *The Plant cell,* **19,** 4077-4090.

Takemoto, D., Rafiqi, M., Hurley, U., Lawrence, G. J., Bernoux, M., Hardham, A. R*., et al.* (2012) N-terminal motifs in some plant disease resistance proteins function in membrane attachment and contribute to disease resistance. *Molecular plant-microbe interactions,* **25,** 379-392.

Torto, T. A., Li, S., Styer, A., Huitema, E., Testa, A., Gow, N. A*., et al.* (2003) EST mining and functional expression assays identify extracellular effector proteins from the plant pathogen Phytophthora. *Genome research,* **13,** 1675-1685.

Van der Biezen, E. A. and Jones, J. D. G. (1998) Plant disease-resistance proteins and the gene-for-gene concept. *Trends in Biochemical Sciences,* **23,** 454-456.

Vleeshouwers, V. G., Rietman, H., Krenek, P., Champouret, N., Young, C., Oh, S. K*., et al.* (2008) Effector genomics accelerates discovery and functional profiling of potato disease resistance and *Phytophthora infestans* avirulence genes. *PloS one,* **3,** e2875.

Win, J., Chaparro-Garcia, A., Belhaj, K., Saunders, D. G., Yoshida, K., Dong, S*., et al.* (2012) Effector biology of plant-associated organisms: concepts and perspectives. *Cold Spring Harbor symposia on quantitative biology,* **77,** 235-247.

Zhang, J., Shao, F., Li, Y., Cui, H., Chen, L., Li, H*., et al.* (2007) A *Pseudomonas syringae* effector inactivates MAPKs to suppress PAMP-induced immunity in plants. *Cell host & microbe,* **11,** 175-185.

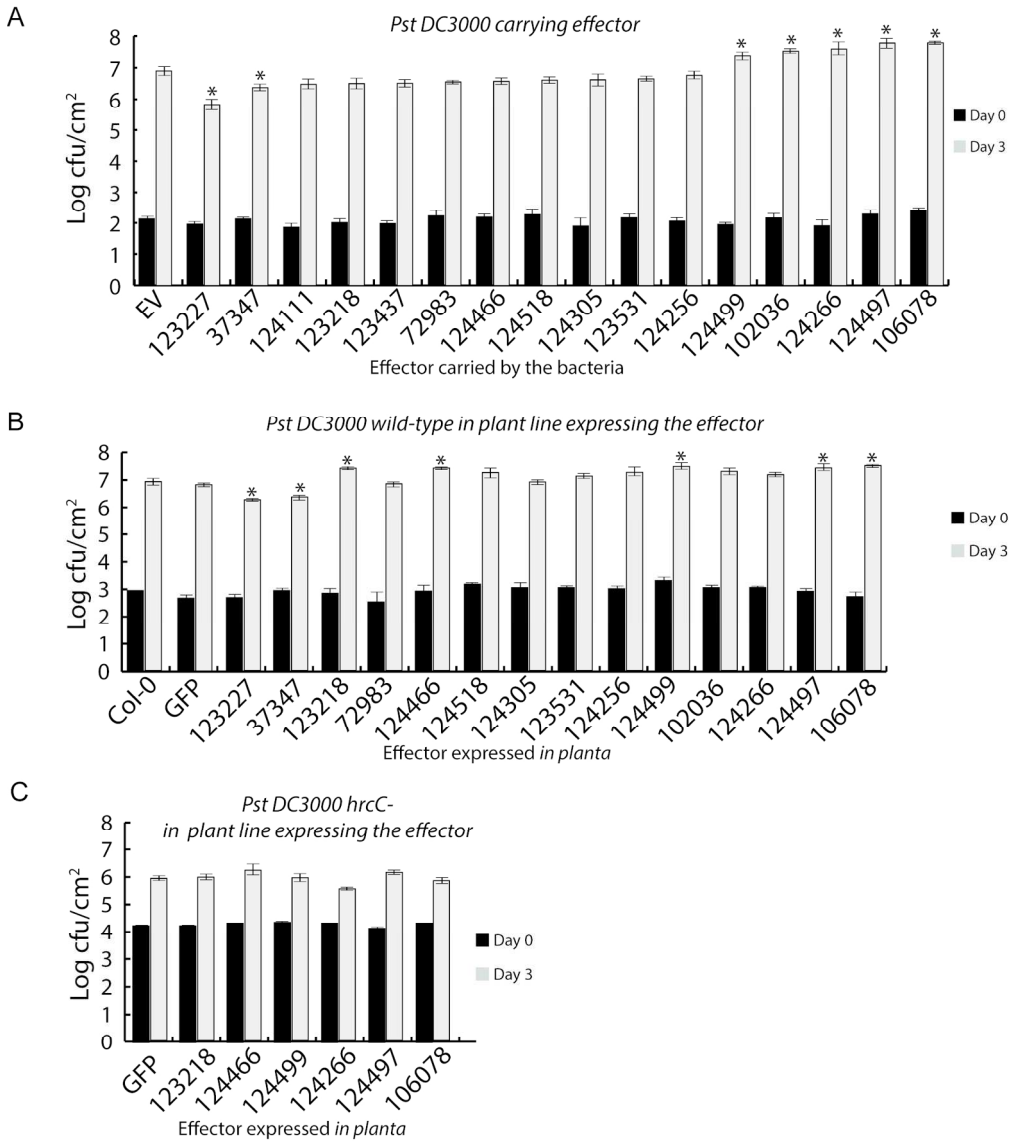

Figure 1. Bacterial growth in planta differs when effectors are delivered by bacteria or constitutively expressed

A) Growth of Pst DC3000 without (EV) or with candidate effectors (all other lanes) was measured on the day of infection and 3 days after infection of 4-week-old plants by leaf infiltration. A bacterial suspension of OD600 = 0.001 was used as inoculum. Statistical significance was evaluated using Student's t-test ($p<0.05$); asterisks indicate statistically significant differences between the effector and empty vector. The experiment was repeated at least three times (a representative experiment is shown).

B) Growth of Pst DC3000 wild-type infecting plants expressing an effector, Col-0 or Col-0 expressing GFP was measured on the day of infection and 3 days after infection of 4-week-old plants by leaf infiltration. A bacterial suspension of OD600 = 0.001 was used as inoculum. Statistical significance was evaluated using Student's t-test ($p<0.05$); asterisk indicates statistically significant difference between plants carrying effector and Col-0 expressing GFP. Five replicates were included for each genotype. To facilitate the comparison with Figure 1A, each transgenic line is presented in the same order as in figure 1A. The experiment was repeated at least three times (a representative experiment is shown).

C) Growth of Pst DC3000 hrcC- strain infecting plants expressing an effector, Col-0 or Col-0 expressing GFP was measured on the day of infection and 3 days after infection of 4-week-old plants by leaf infiltration. A

bacterial suspension of OD600 = 0.001 was used as inoculum. Statistical significance was evaluated using Student's t-test ($p<0.05$); asterisk indicates statistically significant difference between plants carrying effector and Col-0 expressing GFP. Five replicates were included for each genotype. The experiment was repeated at least three times (a representative experiment is shown). Note that no transgenic lines were recovered for 123437 and 124111.

159x180mm (300 x 300 DPI)

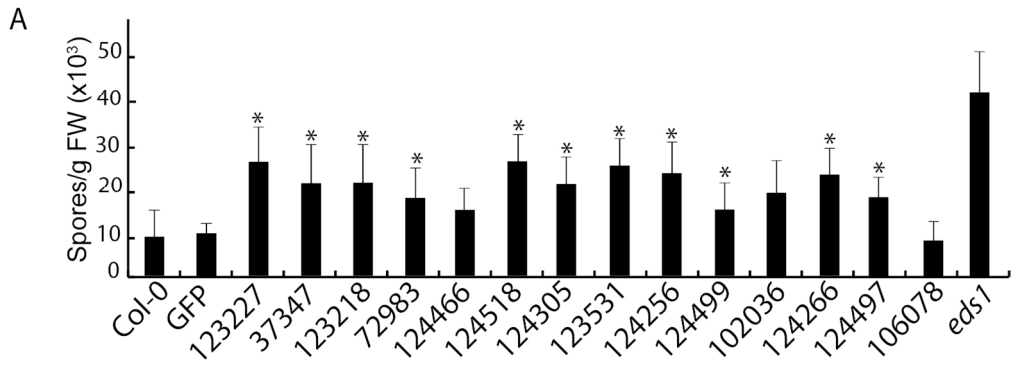

Figure 2. Most candidates effector affect the growth of H.arabidopsidis Noco2 when constitutively expressed in planta.

Two week-old soil-grown plants were inoculated with H. arabidopsidis Noco2 at a concentration of 20,000 conidiospores per ml and the number of conidiospores was quantified 7 days after inoculation. Bars represent the mean of four replicates. Statistical significance was established using Student's t-test ($p<0.05$), and statistically significant differences are represented by an asterisk between plants carrying effector and Col-0 expressing GFP.. Each transgenic line is ordered as in Figure 1 for easier comparison. The experiment was repeated at least five times (representative experiment is shown).

136x49mm (300 x 300 DPI)

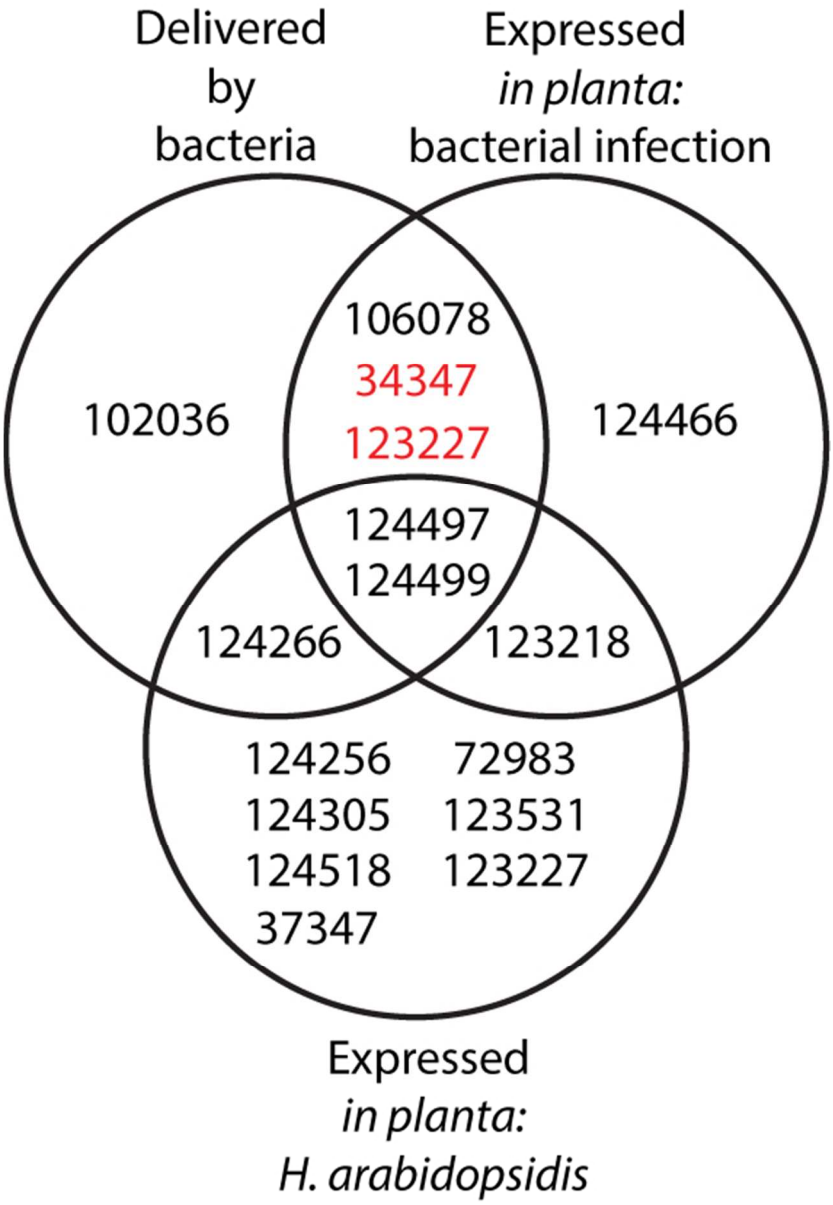

Figure 3. Venn diagram showing the candidate effectors that induced increased virulence (in black) or decreased virulence (in red) .
Note that no transgenic lines were recovered for 123437 and 124111.

48x69mm (300 x 300 DPI)

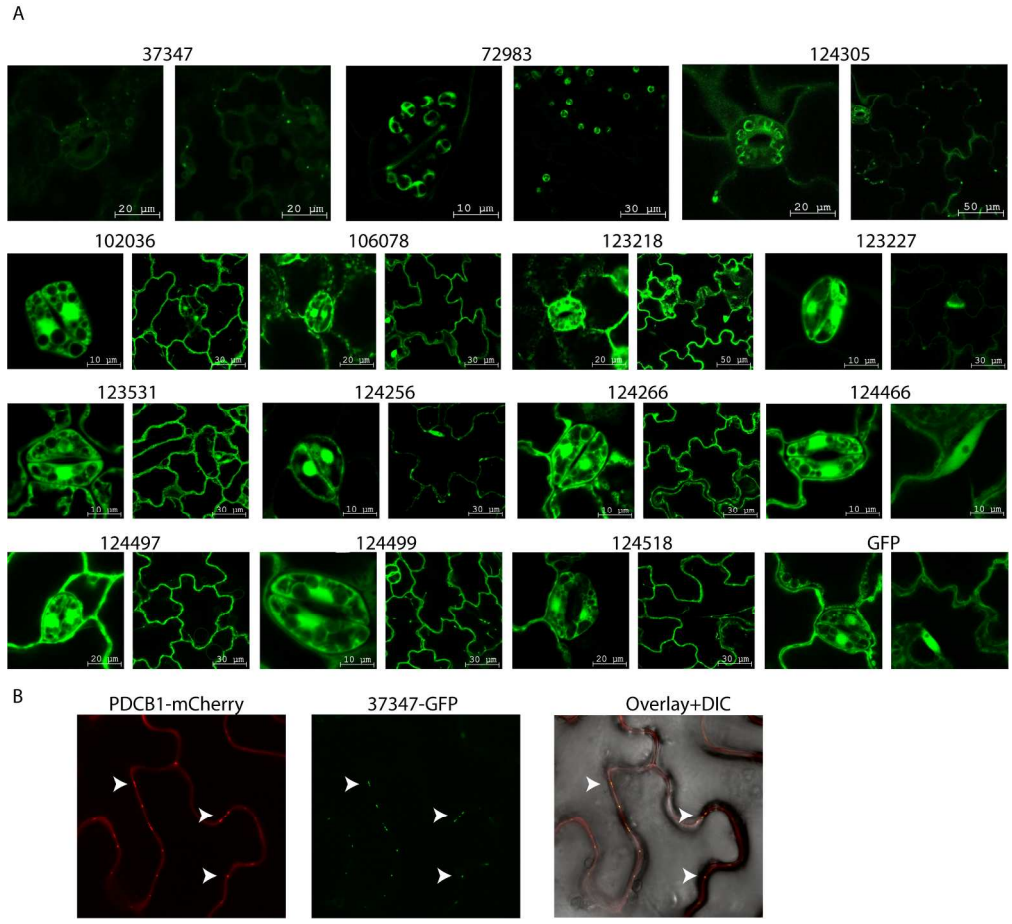

Figure 4. Subcellular localization of the different candidate effectors.
A) Confocal images of leaf epidermal cells of 7 day old transgenic plantlets expressing candidate effectors fused to GFP (SSP-GFP) in Col-0 genetic background. The top three effectors are the ones displaying informative localization, while the bottom three rows display the effectors showing nucleocytoplasmic localization.
B) Colocalization between PDCB1-mCherry , a plasmodesmata marker and 37347-GFP to infer its localization. Left panel red channel, center panel green channel, right panel overlay with DIC.

212x193mm (300 x 300 DPI)